Photocatalytic Oxidation Reactivity of Holes in the Sulfur and Carbon-Doped TiO_2 Powders Studied by Time-Resolved Diffuse Reflectance Spectroscopy

Takashi Tachikawa,[†] Sachiko Tojo,[†] Mamoru Fujitsuka,[†] Teruhisa Ohno,[‡] Kazumoto Nishijima,[‡] Zenta Miyamoto,[‡] and Tetsuro Majima[†,]*

[†] The Institute of Scientific and Industrial Research (SANKEN), Osaka University, Mihogaoka 8-1, Ibaraki, Osaka 567-0047, Japan

[‡] Department of Applied Chemistry, Faculty of Engineering, Kyushu Institute of Technology, Sensuicho 1-1, Tobata, Kitakyushu 804-8550, Japan

Address: The Institute of Scientific and Industrial Research (SANKEN), Osaka University Mihogaoka 8-1, Ibaraki, Osaka 565-0047, Japan

Tel: +81-6-6879-8495

Fax: +81-6-6879-8499

E-mail address: majima@sanken.osaka-u.ac.jp

Abstract: The photocatalytic oxidation reactivities of the photogenerated holes (h^+) during ultraviolet (UV) or visible (Vis) laser flash photolysis of pure anatase, sulfur (S)- and carbon (C)-doped TiO_2 powders were investigated using time-resolved diffuse reflectance (TDR) spectroscopy. The one-electron oxidation processes of substrates, such as methanol (CH_3OH) and 4-(methylthio)phenyl methanol (MTPM), by h^+ at the TiO_2 surface were examined. The TDR spectra and time traces observed for charge carriers and the MTPM radical cation ($MTPM^{\bullet+}$) revealed that the oxidation abilities of h^+ during the 355-nm laser photolysis of TiO_2 powders increased in the order of pure TiO_2 > S-doped TiO_2 >> C-doped TiO_2. On the other hand, no one-electron oxidation reactions of the substrates were observed during the 430-nm laser photolysis of the S- and C-doped TiO_2 powders, although the charge carriers were sufficiently generated upon excitation. The effects of the trapping and detrapping processes of h^+ at the doping sites on the oxidation abilities of the TiO_2 powders were discussed.

1. Introduction

The photocatalytic degradation of pollutants using TiO_2 photocatalysis is attracting considerable attention for applications to environmental problems.[1-6] Typically, the reaction processes are initiated by the band-gap excitation of the TiO_2 particles during ultraviolet (UV) irradiation to generate the oxidizing species, for example, the OH radicals derived from the oxidation of water adsorbed on the surface.[6] However, because of its large band gap of 3.2 eV in the anatase crystalline phase, only the small UV fraction of solar light (about 3–5%) can be utilized. Therefore, many attempts have been made to sensitize TiO_2 for the much larger visible (Vis) fraction.[7-16]

To date, some groups have demonstrated the substitution of a nonmetal atom such as nitrogen (N),[9,10] sulfur (S),[11,12] and carbon (C)[13,14] for oxygen or titanium of TiO_2 or the incorporation of ionic species such as carbonate species into the bulk phase of TiO_2.[15,16] Asahi et al. showed that N doping shifted the absorption edge to a lower energy, thereby increasing the photocatalytic reactivity in the Vis light region.[9] Umebayashi et al. and Ohno et al. fabricated S-doped TiO_2 powders and reported methylene

blue degradation under Vis light irradiation.[11,12] These groups also confirmed that the photocatalyst could decompose 2-propanol to acetone and CO_2 under both UV and Vis light irradiations. On the other hand, C doping in TiO_2 was carried out by the oxidative annealing of TiC.[15] C-doped TiO_2 showed photocatalytic activities for the decomposition of 2-propanol to CO_2 via acetone under Vis light (400–530 nm) irradiation.[15]

Some investigations by product analysis and first-principles calculations for several anion-doped TiO_2 particles proposed that the one of the important factors in the photocatalytic activities is the overlap between the band states of TiO_2, i.e., the hybridization between N, S, and C-derived *p* states and O 2*p* state, to transfer photogenerated charge carriers to reactive sites on the surface of particles.[9] The charge recombination process also plays an important role in the efficiency of the photocatalytic reactions. Hashimoto et al. reported that the quantum efficiency (number of generated acetone molecules / number of absorbed photons) of the decomposition of 2-propanol decreased as the amount of N atoms doped in TiO_2 increased when irradiating with Vis light.[10a] They concluded that this is because the oxygen vacancies, which promote the recombination of holes (h^+) and electrons (e^-), increased with the amount of N atoms doped in the TiO_2. On the other hand, when irradiating with UV light, the quantum efficiency decreased as the concentration of N increased, suggesting that the doping sites could serve as charge recombination centers. Therefore, it is a noteworthy issue to clarify the interfacial electron-transfer reaction dynamics of these charge carriers at the surface. However, only a few quantitative studies have been reported about the photocatalytic reactions of such visualized TiO_2.[17-19] Furthermore, to our knowledge, there are no reports related to these issues using a time-resolved technique.

Time-resolved diffuse reflectance (TDR) spectroscopy is a powerful tool for the investigation of photocatalysis under various conditions.[20-24] Fox and co-workers reported that many oxidation reactions appear to occur by a direct electron transfer from various compounds to the photo-excited TiO_2 powder in CH_3CN.[20] Recently, we studied the one-electron oxidation of several aromatic compounds adsorbed on the surface of the TiO_2 powder slurried in CH_3CN by TDR spectroscopy and concluded that the –OH

and –COOH groups play an important role in the adsorption on the surface of TiO_2 and the efficiency of the one-electron oxidation of aromatic compounds.[24a-c]

In the present study, we investigated the influences of S and C-doping in TiO_2 on the oxidation reaction dynamics of h^+ in the TiO_2 particles using TDR spectroscopy. In order to examine the oxidation reactivity of the photogenerated holes, we used methanol (CH_3OH) and 4-(methylthio)phenyl methanol (MTPM) as substrates. The relationship between the trapping and detrapping processes at the doping sites and the oxidation ability of the photogenerated holes is also discussed.

2. Experimental Section

2.1. Preparation of Pure, S- and C-doped TiO_2. TiO_2 powder (ST-01) was supplied from Ishihara Sangyo along with pure anatase with a BET surface area of 330 m^2 g^{-1} and average primary particle size of 7 nm.

For synthesizing the S-doped TiO_2 powders,[11] titanium isopropoxide (50 g, 0.175 mol) was mixed with thiourea (53.6 g, 0.70 mol) at a molar ratio of 1 to 4 in ethanol (500 mL). The solution was stirred at room temperature for 1 h and completely evaporated under reduced pressure. After evaporation of the ethanol, a white powder was obtained. After calcination at 400 °C under aerated conditions for 3 h, the powder was washed with distilled water. The surface area of the resulting powder was 75.8 m^2/g. The atomic content of S atoms on the surface of the S-doped powder was about 1.6% after the washing treatment, where S^{4+} substitutes for some of the lattice Ti atoms.

A carbonate species-doped TiO_2 (C-doped TiO_2) powder having an anatase phase was prepared as follows.[16] Thiourea (7.6 g) and urea (6.0 g) were mixed with 4.0 g of an anatase TiO_2 powder (ST-01) in an agate mortar. The mixed powder was packed in a capped double alumina crucible and calcined at 400 °C under aerated conditions for 5 h. After calcination, the powder was washed with distilled water. The surface area of the resulting powder was 87.0 m^2/g. The atomic content of C atoms on the surface of the C-doped TiO_2 powder was about 0.4%, where CO_3^{2-} is incorporated into the bulk phase of the TiO_2.

2.2. Chemicals. 4-(Methylthio)phenyl methanol (MTPM) (Aldrich) was purified by vacuum sublimation before use. MTPM has no absorption in the Vis region. Fresh CH_3OH (Nakarai Tesque, spectral grade) was used as the hole scavenger without further purification. Fresh CH_3CN (Nakarai Tesque, spectral grade) was used as the solvent without further purification.

2.3. Instrumentation. The steady-state UV-Vis absorption spectra were measured by an UV-VIS-NIR spectrophotometer (Shimadzu, UV-3100) at room temperature.[23] The sample solutions containing the TiO_2 powder (20 g dm^{-3}) were sonicated for 10 min, and the TiO_2 particles in suspension were then completely removed by centrifugation (10000 rpm, 10 min) using a high-speed microcentrifuge (Hitachi, himac CF16RX) at 22 °C for the UV absorption measurements. All procedures for the sample preparation were performed with shielding from the UV light.

The TDR measurements were performed using the third harmonic generation (355 nm, 5 ns full width at half-maximum) from a Q-switched Nd^{3+}:YAG laser (Continuum, Surelite II-10) and the 430-nm flash from an OPO laser (Continuum, Surelite OPO) pumped by an Nd^{3+}:YAG laser (Continuum, Surelite II-10, 5 ns full width at half-maximum) for the excitation operated with temporal control by a delay generator (Stanford Research Systems, DG535).[24] The reflected analyzing light from a pulsed 450-W Xe-arc lamp (Ushio, XBO-450) was collected by a focusing lens and directed through a grating monochromator (Nikon, G250) to a silicon avalanche photodiode detector (Hamamatsu Photonics, S5343). The transient signals were recorded by a digitizer (Tektronix, TDS 580D). The reported signals are averages of 16-20 events. Sample suspensions were saturated with oxygen gas before irradiation to make the photocatalytic reaction reversible. All experiments were carried out at room temperature.

3. Results

3.1. Photoabsorption of the Pure, S-, and C-doped TiO_2 Powders. The steady-state diffuse reflectance spectra of the S- and C-doped TiO_2 powders, together with a pure anatase TiO_2 powder (ST-01), are shown in Figure 1. Compared to pure anatase TiO_2, the absorption edge was shifted to the

lower-energy region in the spectrum of the S-doped TiO_2 due to the S doping that originates from mixing the S 3*p* states with the valence band (VB), leading to an increase in the VB width as discussed in Section 4.3.[11b] The photoabosorption in the Vis region observed for the C-doped TiO_2 powder is much stronger than that of the S-doped TiO_2 powder, although the atomic content of S atoms on the surface of the S-doped powder is higher than that of C. As presented below, we examined the one-electron oxidation reactivities of h^+ during the 355- and 430-nm laser photolysis of these TiO_2 powders. The absorbance values at 355 nm were 0.72, 0.80, and 0.86 for the pure, S- and C-doped TiO_2 powders, respectively, on the other hand, those at 430 nm were 0.01, 0.19, and 0.48, respectively.

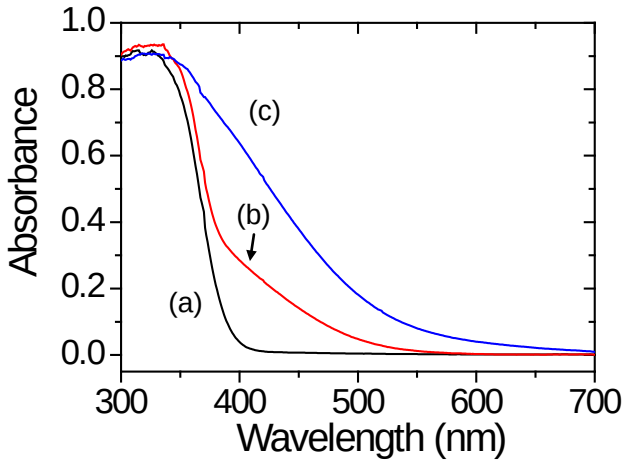

Figure 1. Steady-state diffuse reflectance spectra observed for the pure TiO_2 (a), S- (b), and C-doped (c) TiO_2 powders.

3.2. 355-nm Laser Flash Photolysis of the Pure, S-, and C-doped TiO_2 Powders. We first examined the photogenerated carriers during the 355-nm laser photolysis of the pure, S- and C-doped TiO_2 powders.

Figure 2a shows the TDR spectra observed after the laser flash during the 355-nm laser photolysis (1.5 ± 0.1 mJ $pulse^{-1}$) of the pure TiO_2 powder slurried in O_2-saturated CH_3CN (20 g dm^{-3}). The %absorption (%abs.) is given by eq 1,

$$\%\text{abs.} = \frac{R_0 - R}{R_0} \times 100, \qquad (1)$$

where R and R_0 represent the intensities of the diffuse reflected monitor light with and without excitation, respectively.[24] The linearity for actual absorptions can be satisfied only when %abs. is below 10% as suggested elsewhere.[20,23a]

The broad transient absorption bands with a maximum around 500 nm appeared after the laser flash. The spectral shape was identical within experimental error in the present time period (<30 μs), suggesting that the charge recombination between e^- and h^+ occurred without quenching with some impurities and trapping into other sites.

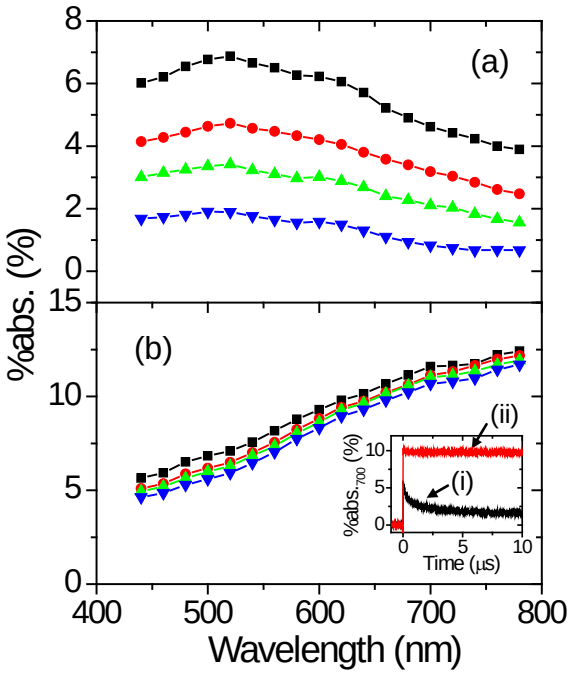

Figure 2. TDR spectra observed at 0.10 (black), 0.5 (red), 2 (green), and 10 (blue) μs after the laser flash during the 355-nm laser photolysis of the pure TiO_2 powder in O_2-saturated CH_3CN (a) and CH_3OH (b). Inset: time traces observed at 700 nm during the 355-nm laser flash photolysis of the pure TiO_2 powder in O_2-saturated CH_3CN (i) and CH_3OH (ii).

As mentioned in the introduction, the valence band hole (h_{VB}^+) and the conduction band electron (e_{CB}^-) are generated in the TiO_2 particles during the band gap excitation (eq 2),

$$TiO_2 \xrightarrow{h\nu} h_{VB}^+ + e_{CB}^- . \qquad (2)$$

The fast charge recombination and transfer kinetics of these photogenerated carriers have been studied in detail by several groups.[25-27] Although most charge carriers quickly recombine, a minority is trapped at the surface of the particles as given by eq 3,

$$h^{+}_{VB} \rightarrow h^{+}_{tr}, e^{-}_{CB} \rightarrow e^{-}_{tr}, \quad (3)$$

where h_{tr}^{+} and e_{tr}^{-} denote the trapped holes and electrons, respectively.

A recent transient absorption study revealed that the absorption spectra of these charge carriers overlap each other in the Vis wavelength range.[28] Thus, a TDR spectrum of h^+ was obtained by subtracting the absorption band of e^- from the observed TDR spectrum. In the presence of CH_3OH as a hole scavenger, the absorption band monotonically increased with the increasing wavelength as shown in Figure 2b.[28-30] This absorption band is mainly due to the free e^- in the TiO_2 particles, because e_{tr}^- localized at the surface of the particles should react very rapidly with oxygen. The decrease in the decay rate of %abs. at 700 nm observed in CH_3OH, compared with that in CH_3CN, strongly supports the fact that the recombination processes between e^- and h^+ are inhibited by the scavenging of h^+ at the surface of the TiO_2 powder as given by eq (4),[31,32]

$$CH_3O^{-}_{ads} + h^{+} \rightarrow CH_3O^{\bullet}_{ads}. \quad (4)$$

The generated methoxy radical then decomposes and the radical anion intermediate ($CH_2O_{ads}^{\bullet -}$) adsorbed on the surface injects an electron into the CB of TiO_2 as given by eqs (5)-(6),[33]

$$CH_3O^{\bullet}_{ads} \rightarrow CH_2O^{\bullet -}_{ads} + H^{+}, \quad (5)$$

$$CH_2O^{\bullet -}_{ads} \rightarrow CH_2O_{ads} + e^{-}. \quad (6)$$

An increase in %abs. at 700 nm due to the injected electron, however, was not observed on our time scale from 50 ns to 30 μs. The absence of the expected rise shows that the electron injection was completed within the laser duration (5 ns) as reported elsewhere.[31]

Figure 3a shows the difference TDR spectra obtained by subtracting the TDR spectrum observed at 10 μs after the laser flash during the 355-nm laser photolysis of pure TiO_2 powder in O_2-saturated CH_3OH from the TDR spectra observed at 0.10 (black), 0.5 (red), 2 (green), and 10 (blue) μs after the laser flash

during the 355-nm laser photolysis of pure TiO_2 powder in CH_3CN. The %abs. values were normalized at 780 nm for each subtraction, because those at 780 nm are mainly due to e^-. As shown in the inset of Figure 3a, a broad transient absorption band with a maximum around 500-520 nm was obtained and was quite identical with the absorption band of h_{tr}^+.[28]

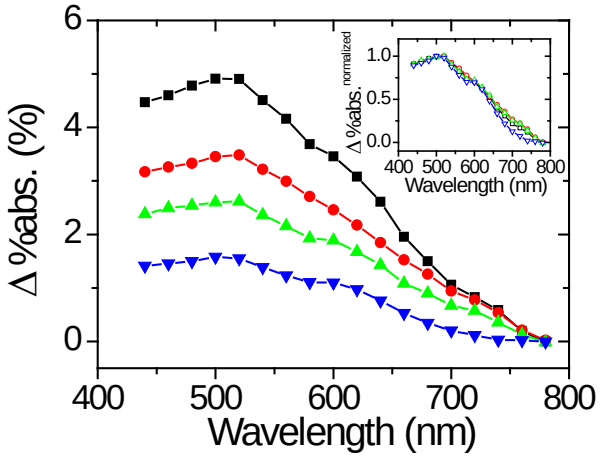

Figure 3. Difference TDR spectra obtained from subtracting TDR spectrum observed at 10 μs after the laser flash during the 355-nm laser photolysis of the pure TiO_2 powder in O_2-saturated CH_3OH from TDR spectra observed at 0.10 (black), 0.5 (red), 2 (green), and 10 (blue) μs after the laser flash during the 355-nm laser photolysis of the pure TiO_2 powder in O_2-saturated CH_3CN, where %abs. values were normalized at 780 nm for each subtractions. Inset: normalized difference TDR spectra.

Similar procedures were applied for the S- and C-doped TiO_2 in order to assign the absorption bands of the photogenerated charge carriers.

Figures 4a and b show the TDR spectra observed after the laser flash during the 355-nm laser photolysis of the S-doped TiO_2 powder slurried in O_2-saturated CH_3CN and CH_3OH, respectively. Compared with pure TiO_2, significant changes in the spectral shapes were observed. The absorption band around 440-650 nm attributed to h_{tr}^+ was much smaller than that around 700-780 nm attributed to e^-. It should also be noted that the absorption band due to h_{tr}^+ disappeared in the nanosecond time domain as shown in Figure 4a, while the absorption band due to e^- showed no significant change in the

decay kinetics. These results clearly suggest that the h_{tr}^+, which shows the absorption band around 440-650 nm, is detrapped and then trapped at other sites which have no absorption in the present wavelength region (440-780 nm). The h_{tr}^+ was also quickly scavenged by CH_3OH analogous to the pure TiO_2 powder as shown in Figure 4b.

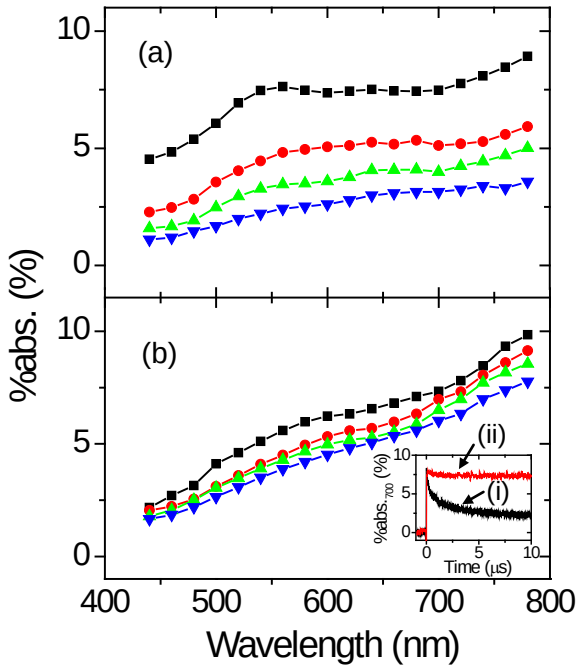

Figure 4. TDR spectra observed at 0.1 (black), 0.5 (red), 2 (green), and 10 (blue) μs after the laser flash during the 355-nm laser photolysis of the S-doped TiO_2 powder in O_2-saturated CH_3CN (a) and CH_3OH (b). Inset: time traces observed at 700 nm during the 355-nm laser flash photolysis of the S-doped TiO_2 powder in O_2-saturated CH_3CN (i) and CH_3OH (ii).

Figures 5a and b show the TDR spectra observed after the laser flash during the 355-nm laser photolysis of the C-doped TiO_2 powder slurried in O_2-saturated CH_3CN and CH_3OH, respectively. The observed spectral shapes in CH_3CN were similar to those of the S-doped TiO_2, although no fast decay components were observed. On the other hand, the oxidation reaction dynamics of the C-doped TiO_2 is quite different from the other TiO_2 powders. As shown in the inset of Figure 5b, a relatively slow decay component in the nanosecond time domain was observed at 700 nm during the 355-nm laser flash

photolysis of the C-doped TiO_2 powder in CH_3OH (trace (ii)). In the case of pure TiO_2, a large number of h^+ were scavenged by CH_3OH within the laser duration (5 ns) as shown in the inset of Figure 2b. The quenching effects of h^+ by CH_3OH increased in the order of the pure > S-doped >> C-doped TiO_2, suggesting that the rates of trapping and detrapping are quite different from each other.

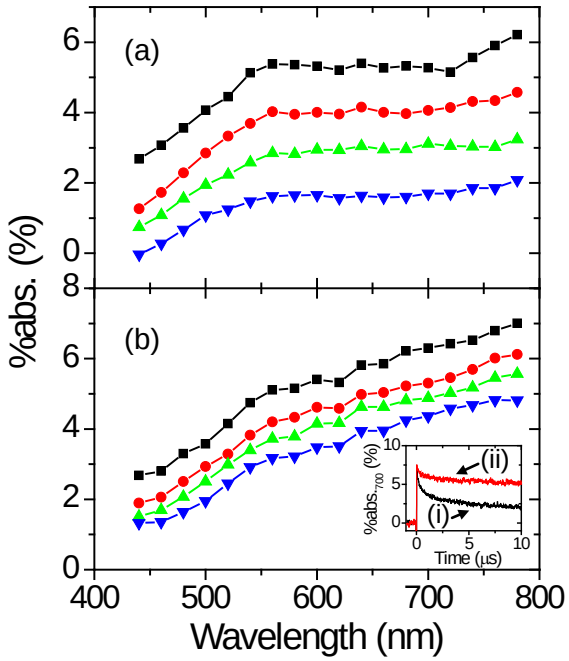

Figure 5. TDR spectra observed at 0.1 (black), 0.5 (red), 2 (green), and 10 (blue) μs after the laser flash during the 355-nm laser photolysis of the C-doped TiO_2 in O_2-saturated CH_3CN (a) and CH_3OH (b). Inset: time traces observed at 700 nm during the 355-nm laser flash photolysis of the C-doped TiO_2 powder in O_2-saturated CH_3CN (i) and CH_3OH (ii).

To examine the oxidation power of pure, S- and C-doped TiO_2 powders, we used MTPM, which has an oxidation potential (E_{ox}) of 1.59 V vs. NHE, as a hole acceptor.[24a,c]

In the present systems, we assumed that h_{VB}^+ and/or h_{tr}^+ are the main oxidizing species as given by eq 7,

$$h_{VB}^+ (h_{tr}^+) + \mathrm{MTPM} \rightarrow \mathrm{MTPM}^{\bullet +}. \quad (7)$$

where h_{VB}^+ has a flat band potential for the valence band (E_{VB}) of +2.1 V vs. NHE.[34]

Figure 6a-c show the TDR spectra obtained during the 355-nm laser photolysis of pure (a), S- (b), and C-doped (c) TiO_2 powders in the presence of MTPM (1×10^{-2} mol dm^{-3}) in O_2-saturated CH_3CN. As

shown in Figure 6c, the transient absorption band at 500 – 700 nm was obtained and assigned to the MTPM radical cation ($MTPM^{\bullet+}$), although the spectral shape was approximately 1.5 times broader than that obtained during the pulse radiolysis of the N_2O-saturated aqueous solution in the presence of MTPM.[35-37] Figure 6d also shows the difference TDR spectra obtained by subtracting the TDR spectrum observed at 10 μs after the laser flash during the 355-nm laser photolysis of the corresponding powders in CH_3OH from the TDR spectra observed at 0.05 μs after the laser flash during the 355-nm laser photolysis of the pure (closed squares), S- (closed circles), and C-doped (closed triangles) TiO_2 powders in CH_3CN, in which the %abs. values were normalized at >720 nm for each subtraction. The amounts of the generated $MTPM^{\bullet+}$ increased in the order of pure > S-doped >> C-doped TiO_2. Recently, we found that the initial concentration of the radical cations generated from the one-electron oxidation reaction with h^+ significantly depends on the amount of substrates adsorbed on the surface.[24a-c] From the steady-state UV absorption measurements, the amounts of MTPM adsorbed on the surface of 1.6, 1.1, and 1.3 × 10^{-4} mol g^{-1} were determined for the pure, S-, and C-doped TiO_2 powders, respectively. Considering the amounts of MTPM adsorbed on the surface of the TiO_2 powders, therefore, the efficiency of the one-electron oxidation of MTPM by h^+ increased in the order of pure > S-doped > C-doped TiO_2. For example, the amount of $MTPM^{\bullet+}$ observed for pure TiO_2 is about three times greater compared with that for the C-doped TiO_2, suggesting that the apparent one-electron oxidation ability of the C-doped TiO_2 is quite lower than pure TiO_2.

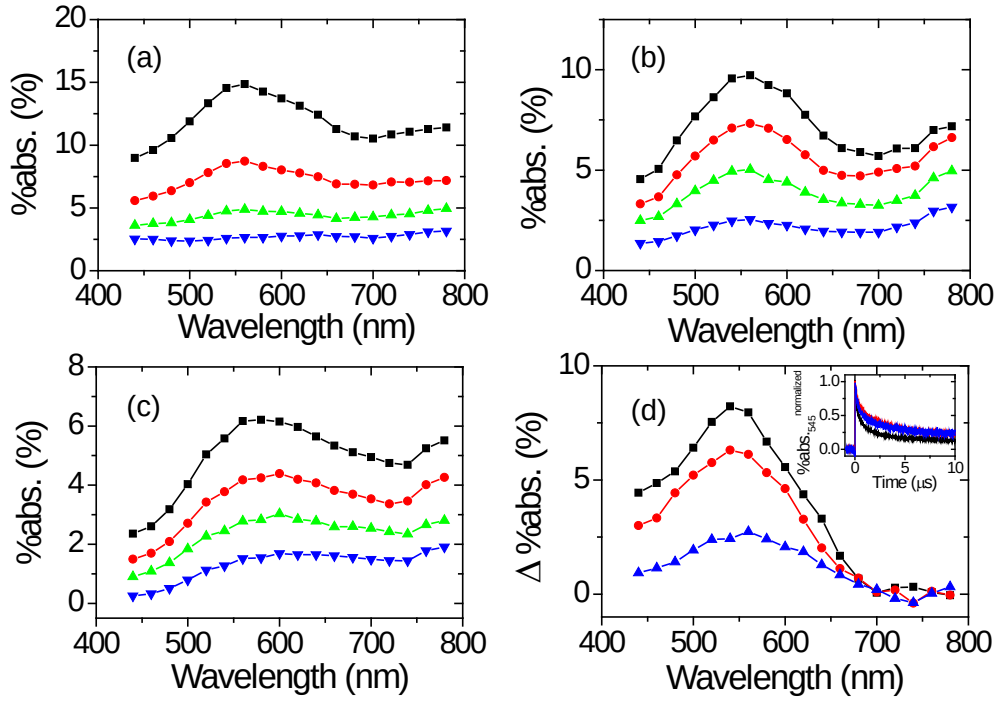

Figure 6. TDR spectra observed at 0.1 (black), 0.5 (red), 2 (green), and 10 (blue) μs after the laser flash during the 355-nm laser photolysis of the pure (a), S- (b), and C-doped (c) TiO_2 powders in the presence of MTPM (1×10^{-2} mol dm^{-3}) in O_2-saturated CH_3CN. Difference TDR spectra were obtained from subtracting the TDR spectrum observed at 10 μs after the laser flash during the 355-nm laser photolysis of the pure, S-, and C-doped TiO_2 powders in O_2-saturated CH_3OH from the TDR spectra observed at 0.05 μs after the laser flash during the 355-nm laser photolysis of the pure (closed squares), S- (closed circles), and C-doped (closed triangles) TiO_2 powders in O_2-saturated CH_3CN, where %absorption values were normalized at >720 nm for each subtraction. Open circles denote the normalized difference TDR spectrum observed for the S- (circles) and C-doped (triangles) TiO_2. Inset: time traces observed at 545 nm during the 355-nm laser flash photolysis of the pure (black), S- (red), and C-doped (blue) TiO_2 powders in the presence of MTPM (1×10^{-2} mol dm^{-3}) in O_2-saturated

3.3. 430-nm Laser Flash Photolysis of the S- and C-doped TiO_2 Powders. Next, we examined the photogenerated carriers during the 430-nm laser photolysis of the S- and C-doped TiO_2 powders.

Figures 7a and b show the TDR spectra observed after the laser flash during the 430-nm laser photolysis (1.8 ± 0.3 mJ pulse^{-1}) of the S-doped TiO_2 powder in O_2-saturated CH_3CN and CH_3OH, respectively. No significant difference in the spectral shapes was observed in CH_3CN and CH_3OH, although slight difference of a few % in absorption was observed. As shown in Figure 7c, almost the same time profiles at 700 nm indicate the poor reactivity of h^+ with CH_3OH during the 430-nm laser photolysis of the S-doped TiO_2 powder compared with the 355-nm laser excitation (inset of Figure 4b). We also examined the one-electron oxidation of MTPM during the 430-nm laser photolysis of the S-doped TiO_2 powder as shown in Figure 7d. The transient absorption band assigned to $MTPM^{\bullet+}$ was observed, however, it would be attributable to $MTPM^{\bullet+}$ generated by the direct excitation of the charge transfer complex between MTPM and TiO_2.[23b] These experimental results suggest that a large number of h_{tr}^+ are localized in the particles and not at the surface of the particles during the 430-nm laser photolysis of the S-doped TiO_2 powder.

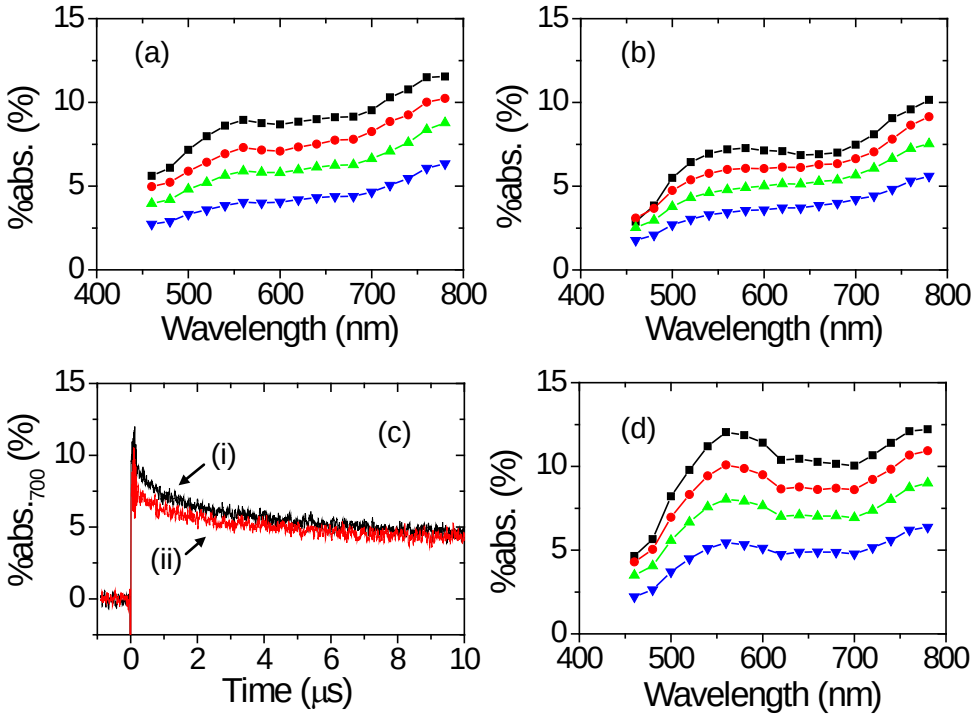

Figure 7. TDR spectra observed at 0.1 (black), 0.5 (red), 2 (green), and 10 (blue) μs after the laser flash during the 430-nm laser photolysis of the S-doped TiO_2 powder in O_2-saturated CH_3CN (a) and CH_3OH (b). Time traces observed at 700 nm during the 430-nm laser flash photolysis of the S-doped TiO_2 powder in O_2-saturated CH_3CN (i) and CH_3OH (ii) (c). TDR spectra observed at 0.1 (black), 0.5 (red), 2 (green), and 10 (blue) μs after the laser flash during the 430-nm laser photolysis of the S-doped TiO_2 powder in the presence of MTPM (1×10^{-2} mol dm^{-3}) in O_2-saturated CH_3CN (d).

Figures 8a and b also show the TDR spectra observed after the laser flash during the 430-nm laser photolysis of the C-doped TiO_2 powder in O_2-saturated CH_3CN and CH_3OH, respectively. A similar tendency to the S-doped TiO_2 was observed. No significant difference in the spectral shapes was observed in CH_3CN (a) and CH_3OH (b), although a slight difference in %abs. was observed. As shown in Figure 8c, almost the same time profiles at 700 nm support the poor reactivity of h^+ with CH_3OH during the 430-nm laser photolysis of the C-doped TiO_2 powder, compared with the 355-nm laser excitation (inset of Figure 5b). No one-electron oxidation of MTPM occurred as shown in Figure 7d.

These results suggest that the major part of the trapped h^+ is also localized in the particles, not at the surface of the particles during the 430-nm laser photolysis of the C-doped TiO_2 powder analogous to the S-doped TiO_2.

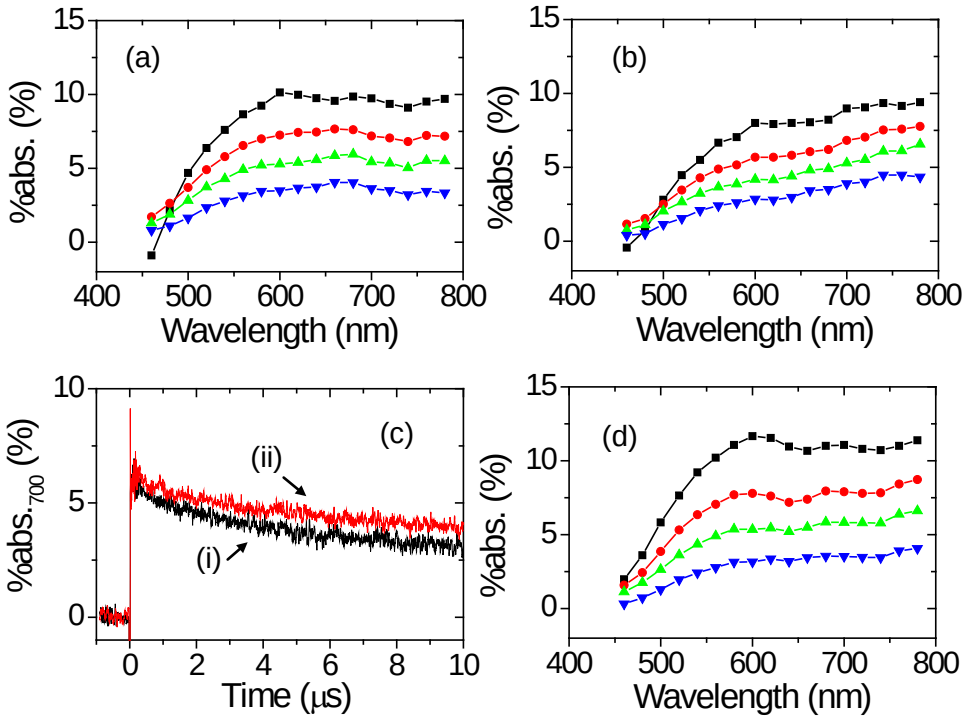

Figure 8. TDR spectra observed at 0.1 (black), 0.5 (red), 2 (green), and 10 (blue) μs after the laser flash during the 430-nm laser photolysis of the C-doped TiO_2 powder in O_2-saturated CH_3CN (a) and CH_3OH (b). Time traces observed at 700 nm during the 430-nm laser flash photolysis of the C-doped TiO_2 powder in O_2-saturated CH_3CN (i) and CH_3OH (ii) (c). TDR spectra observed at 0.1 (black), 0.5 (red), 2 (green), and 10 (blue) μs after the laser flash during the 430-nm laser photolysis of the C-doped TiO_2 powder in the presence of MTPM (1×10^{-2} mol dm^{-3}) in O_2-saturated CH_3CN (d).

4. Discussion

4.1 Efficiency of the Generation of Charge Carriers

We would like to first discuss the efficiency of the generation of charge carriers during the 355- and 430-nm laser photolyses of the pure, S- and C-doped TiO_2 powders. The absorbed photon numbers (N_p) and initial %abs. (%abs.$^{t=0}$) values observed at 780 nm during the 355- and 430-nm laser flash photolyses of the pure, S- and C-doped TiO_2 powders in O_2-saturated CH_3CN are summarized in Table 1. Here, we defined the efficiency factor (*f*) for the carrier generations as %abs.$^{t=0}/N_p$ for comparison.

The relatively large *f* values obtained during the 430-nm laser photolysis of the S- and C-doped TiO_2 powders should be noted. As discussed in the next section, the recombination rates of the charge carriers during the 355-nm excitation were higher than those during the 430-nm excitation. These results suggest that relatively large *f* values obtained for the 430-nm excitation are mainly attributable to the suppression of the charge recombination process due to the slow migration of carriers in the particles.

Table 1. Absorbed photon number (N_p) and initial %abs. (%abs.$^{t=0}$) observed at 780 nm during the 355- and 430 nm laser flash photolysis of the pure, S-, and C-doped TiO_2 powders in O_2-saturated CH_3CN

wavelength, nm [a]	TiO_2	N_p, 10^{15} (rel.)	%abs$^{t=0}$, % [b] (rel.)	*f*, 10^{-17} [c] (rel.)
355	pure	2.2 (1.0)	5.5 (1.0)	2.5 (1.0)
	S-doped	2.3 (1.0)	12.0 (2.8)	5.2 (2.1)
	C-doped	2.3 (1.0)	8.3 (1.5)	3.6 (1.4)
430	S-doped	1.4 (0.65)	14.5 (2.6)	10.4 (4.1)
	C-doped	2.6 (1.2)	13.0 (2.4)	5.0 (2.0)

[a] Wavelength of the excitation laser. [b] Observed at 780 nm. [c] Calculated from %abs$^{t=0}/N_p$.

4.2 Charge Recombination Processes

As shown in the inset of Figure 2, the time profile observed for the pure TiO_2 in CH_3CN cannot be fit by a simple single-exponential decay function. The nonexponential decay profile of recombination can be explained by using the model of recombination kinetics based on detrapping from deep traps.[38] Therefore, the observed nonexponential decay kinetics clearly indicates that the recombination rates are limited by the motion of e^- and h^+ in the particles. As suggested elsewhere, the recombination time has

been evaluated as the time required for 50% of the initial %abs. values ($t_{1/2}$).[28,38] The determined $t_{1/2}$ values for the pure, S-, and C-doped TiO_2 are summarized in Table 2. For the 355-nm excitation, the $t_{1/2}$ values of 0.9, 1.5, and 1.6 μs at 700 nm were determined for the pure, S-, and C-doped TiO_2 in CH_3CN, respectively, suggesting that the doping sites *do not* serve as charge recombination centers and the motions of e^- and h^+ depend on the nature of each TiO_2 powder. As we discussed above, the recombination rates should be limited by the effective mobility of the charge carriers. Therefore, the differences in the driving force and reorganization energy for the charge-transfer reaction are not the reason for the large difference in $t_{1/2}$ obtained for each TiO_2 powder. On the other hand, the $t_{1/2}$ values of 0.35, 1.2, and 0.85 μs at 545 nm were observed for the pure, S-, and C-doped TiO_2 in the presence of MTPM in CH_3CN. These values are almost half of those determined for the recombination between e^- and h^+. As is well-known, the time profiles of the recombination are strongly affected by the light intensity. This observation is interpreted in terms of a trap-filling effect.[38,39] That is, the generated electrons are immediately trapped, and they occupy deep traps in the particles. Therefore, the effective mobility of the other electrons increases. In fact, a slow recombination was observed under weak excitation conditions.[27] In the presence of MTPM, a considerable number of e^- were generated in particles as shown in Figure 6a, compared with that in the absence of MTPM (see Figure 2a), and as a result, the recombination process between e^- and $MTPM^{\bullet+}$ was enhanced. Thus, the difference in $t_{1/2}$ between h^+ and $MTPM^{\bullet+}$ may be due to the number of electrons generated by the charge separation.

It is noteworthy that the $t_{1/2}$ values determined for the pure, S-, and C-doped TiO_2 under the 430-nm excitation are significantly higher than the 355-nm excitation in spite of the generation of the number of charge carriers, compared with the 355-nm excitation. It appears that the suppression of the charge recombination process under the 430-nm excitation is due to the low mobility of h^+ in the particles.

Table 2. Half times for charge recombination ($t_{1/2}$) observed during the 355- and 430 nm laser flash photolysis of the pure, S-, and C-doped TiO_2 powders in the absence and presence of MTPM (1×10^{-2} mol dm^{-3}) in O_2-saturated CH_3CN

wavelength, nm [a]	TiO_2	substrate	$t_{1/2}$, μs
355	pure	non	0.9 ± 0.2 [b]
	S-doped	non	1.5 ± 0.2 [b]
	C-doped	non	1.6 ± 0.2 [b]
	pure	MTPM	0.4 ± 0.1 [c]
	S-doped	MTPM	1.1 ± 0.2 [c]
	C-doped	MTPM	0.9 ± 0.1 [c]
430	S-doped	non	10 ± 1 [b]
	C-doped	non	9.0 ± 1 [b]

[a] Wavelength of the excitation laser. [b] Observed at 700 nm. [c] Observed at 545 nm.

4.3. Mechanisms of the Photocatalytic Oxidation Reactions. No significant difference in the amount of adsorbates was observed for the pure, S- and C-doped TiO_2 powders as mentioned in Section 3.1. Therefore, we considered that the remarkable differences in the photocatalytic oxidation reactivity are mainly due to the charge separation and recombination processes.

In the case of pure TiO_2, when irradiating with UV light, the generated h^+ is quickly trapped on the surface of the particles and react with adsorbates as shown in Figure 9a. On the other hand, in the case of the S- and C-doped TiO_2 particles, the generated h^+ are trapped in the particles and on the surface of particles under UV excitation (Figure 9b). When irradiating with Vis light, the generated h^+ in the S- and C-doped TiO_2 particles are quickly trapped in deep trapping sites, that is, doping sites, although we cannot directly observe its absorption band. This h_{tr}^+ should have a poor reactivity because of its low E_{ox} compared with those of adsorbates. Our experimental results are quite consistent with those reported by Nakato et al..[19] They concluded that photocatalytic oxidation of organic compounds on N-doped TiO_2 under Vis illumination mainly proceed via reactions with surface intermediates of water oxidation or oxygen reduction, not by direct reactions with holes trapped at the N-induced midgap level.[19]

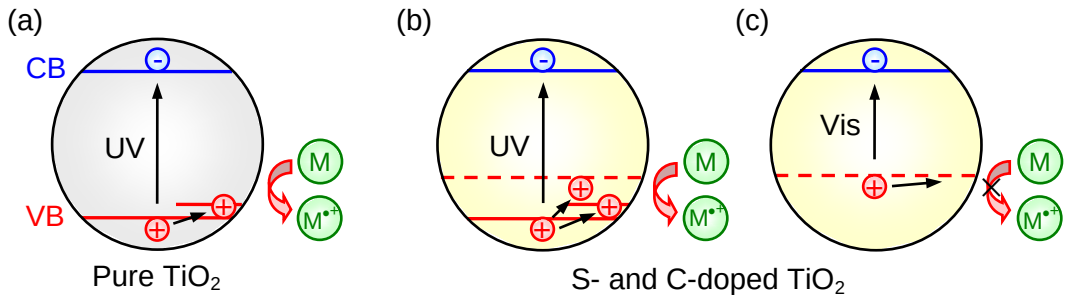

Figure 9. Photocatalytic one-electron oxidation process of organic molecule (M) adsorbed on the surfaces of the pure (a), S-, and C-doped (b and c) TiO_2 particles. Minus and plus signs denote e^- and h^+. The CB and VB denote the valence band and the conduction band of the TiO_2 particles, respectively. Short solid lines indicate the trapping sites. Broken lines indicate the S- and C-induced

Based on the theoretical analyses using *ab initio* band calculations, the VB and CB consist of both Ti 3*d* and O 2*p* orbitals in the pure anatase TiO_2 crystal.[9a] When TiO_2 is doped with S, the S 3*p* states are somewhat delocalized, thus greatly contributing to the formation of the VB with the O2*p* and Ti 3*d* states (see Figure 5 in Ref. 11b). This interaction between the S 3*p* and O 2*p* states would influence the trapping and detrapping process, that is, a hole migration, in the particles. On the other hand, in the case of the C-doped TiO_2, no contribution of C *p* was expected on the O 2*p* states.[9a] Unfortunately, we cannot discuss the effect on the hole migration and the oxidation reactivity of the C-doped TiO_2, because we have no data for the band structure of the present carbonate species-doped TiO_2. However, the fact is that the inefficient h^+ scavenging by CH_3OH during the 355- and 430-nm laser photolyses of the C-doped TiO_2 powder would be attributable to the trapping of h^+ at the doping sites electrically separated from O 2*p* states of TiO_2. It seems that the trapping and detrapping processes play an important role in the photocatalytic activity of the S- and C-doped TiO_2 powders.

5. Conclusions

We have investigated the photocatalytic oxidation power of the photogenerated holes during the UV or Vis laser flash photolysis of S- and C-doped TiO_2 powders using TDR spectroscopy. The oxidation abilities of h^+ generated during the 355-nm laser photolysis of the TiO_2 powders increased in the order of pure > S >> C. On the other hand, no oxidation reaction was observed during the 430-nm laser photolysis of the S- and C-doped TiO_2 powders, although the charge carriers were sufficiently generated under excitation. The trapping of h^+ at the doping sites to prevent the hole migration would be a crucial process for the oxidation ability of the S- and C-doped TiO_2 powders.

Acknowledgment. This work has been partly supported by a Grant-in-Aid for Scientific Research on Priority Area (417), 21st Century COE Research, and others from the Ministry of Education, Culture, Sports, Science and Technology (MEXT) of the Japanese Government.

References and Notes

(1) Fujishima, A.; Rao, T. N.; Tryk, D. A. *J. Photochem. Photobiol. C: Photochem. Rev.* **2000**, *1*, 1.

(2) Mills, A.; Hunte, S. L. *J. Photochem. Photobiol. A* **1997**, *108*, 1.

(3) Serpone, N.; Pelizzetti, E.; Hidaka, H. In Photocatalytic Purification and Treatment of Water and Air; Ollis, D. F., Al-Ekabi, H., Eds.; Elsevier: London, 1993; pp 225-250.

(4) Fox, M. A.; Dulay, M. T. *Chem. Rev.* **1993**, *93*, 341.

(5) Linsebigler, A. L.; Lu, G.; Yates, Jr., Y. T. *Chem. Rev.* **1995**, *95*, 735.

(6) Hoffmann, M. R.; Martin, S. T.; Choi, W.; Bahnemann, D. W. *Chem. Rev.* **1995**, *95*, 69.

(7) Sato, S. *Chem. Phys. Lett.* **1986**, *123*, 126.

(8) Noda, H.; Oikawa, K.; Ogata, T.; Matsuki, K.; Kamata, H. *Chem. Soc. Jpn.* **1986**, *8*, 1084.

(9) (a) Asahi, R.; Morikawa, T.; Ohwaki, T.; Aoki, K.; Taga, Y. *Science* **2001**, *293*, 269. (b) Morikawa, T.; Asahi, R.; Ohwaki, T.; Aoki, K.; Taga, Y. *Jpn. J. Appl. Phys.* **2001**, *40*, L561.

(10) (a) Irie, H.; Watanabe, Y.; Hashimoto, K. *J. Phys. Chem. B* **2003**, *107*, 5483. (b) Miyauchi, M.; Ikezawa, A.; Tobimatsu, H.; Irie, H.; Hashimoto, K. *Phys. Chem. Chem. Phys* **2004**, *6*, 865.

(11) (a) Ohno, T.; Mitsui, T.; Matsumura, M. *Chem. Lett.* **2003**, *32*, 364. (b) Ohno, T.; Akiyoshi, M.; Umebayashi, T.; Asai, K.; Mitsui, T.; Matsumura, M. *Appl. Catal.* **2004**, *265*, 115.

(12) (a) Umebayashi, T.; Yamaki, T.; Itoh, H.; Asai, K. *Appl. Phys. Lett.* **2002**, *81*, 454. (b) Umebayashi, T.; Yamaki, T.; Tanaka, S.; Asai, K. *Chem. Lett.* **2003**, *32*, 330.

(13) Khan, S. U. M.; Al-Shahry, M.; Ingler, W. B. J. *Science* **2002**, *297*, 2243.

(14) Irie, H.; Watanabe, Y.; Hashimoto, K. *Chem. Lett.* **2003**, *32*, 772.

(15) Sakthivel, S.; Kisch, H. *Angew. Chem. Int. Ed.* **2003**, *42*, 4908.

(16) Ohno, T.; Tsubota, T.; Nishijima, K.; Miyamoto, Z. *Chem. Lett.* **2004**, *33*, 2.

(17) (a) Diwald, O.; Thompson, T. L.; Zubkov, T.; Goralski, Ed. G.; Walck, S. D.; Yates, Jr., J. T. *J. Phys. Chem. B* **2004**, *108*, 6004. (b) Diwald, O.; Thompson, T. L.; Goralski, Ed. G.; Walck, S. D.; Yates, Jr., J. T. *J. Phys. Chem. B* **2004**, *108*, 52.

(18) Torres, G. R.; Lindgren, T.; Lu, J.; Granqvist, C. –G.; Lindquist, S. –E. *J. Phys. Chem. B* **2004**, *108*, 5995.

(19) Nakamura, R.; Tanaka, T.; Nakato, Y.; *J. Phys. Chem. B* in press.

(20) (a) Kessler, R. W.; Krabichler, G.; Uhl, S.; Oelkrug, D.; Hagan, W. P.; Hyslop, J.; Wilkinson, F. *Opt. Acta* **1983**, *30*, 1099. (b) Oelkrug, D.; Honnen, W.; Wilkinson, F.; Willsher, C. J. *J. Chem. Soc. Faraday Trans. II* **1987**, *83*, 2081.

(21) (a) Draper, R. B.; Fox, M. A. *J. Phys. Chem.* **1990**, *94*, 4628. (b) Draper, R. B.; Fox, M. A. *Langmuir* **1990**, *6*, 1396. (c) Fox, M. A.; Dulay, M. T. *J. Photochem. Photobiol. A: Chem.* **1996**, *98*, 91.

(22) (a) Colombo, Jr., D. P.; Bowman, R. M. *J. Phys. Chem.* **1995**, *99*, 11752. (b) Colombo, Jr., D. P.; Bowman, R. M. *J. Phys. Chem.* **1996**, *100*, 18445.

(23) (a) Asahi, T.; Furube, A.; Fukumura, H.; Ichikawa, M.; Masuhara, H. *Rev. Sci. Instrum.* **1998**, *69*, 361. (b) Furube, A.; Asahi, T.; Masuhara, H.; Yamashita, H.; Anpo, M. *J. Phys. Chem. B* **1999**, *103*, 3120. (c) Furube, A.; Asahi, T.; Masuhara, H.; Yamashita, H.; Anpo, M. *Res. Chem. Intermed.* **2001**, *27*, 177.

(24) (a) Tachikawa, T.; Tojo, S.; Fujitsuka, M.; Majima, T. *Chem. Phys. Lett.* **2003**, *382*, 618. (b) Tachikawa, T.; Tojo, S.; Fujitsuka, M.; Majima, T. *Langmuir* **2004**, *20*, 2753. (c) Tachikawa, T.; Tojo, S.; Fujitsuka, M.; Majima, T. *J. Phys. Chem. B* **2004**, *108*, 5859. (d) Tachikawa, T.; Tojo, S.; Fujitsuka, M.; Majima, T. *Langmuir* **2004**, *20*, 4327. (e) Tachikawa, T.; Tojo, S.; Fujitsuka, M.; Majima, T. *Tetrahedron Lett.* **2004**, *45*, 3753. (f) Tachikawa, T.; Tojo, S.; Fujitsuka, M.; Majima, T. *Chem. Phys. Lett.* **2004**, *392*, 50. (g) Tachikawa, T.; Tojo, S.; Fujitsuka, M.; Majima, T. *J. Phys. Chem. B* in press.

(25) Rothenberger, G..; Moser, J.; Grätzel, M.; Serpone, N.; Sharma, D. K. *J. Am. Chem. Soc.* **1985**, *107*, 8054.

(26) Serpone, N.; Lawless, D.; Khairutdinov, R.; Pelizzetti, E. *J. Phys. Chem.* **1995**, *99*, 16655.

(27) Bahnemann, D. W.; Hilgendorff, M.; Memming, R. *J. Phys. Chem. B* **1997**, *101*, 4265.

(28) Yoshihara, T.; Katoh, R.; Furube, A.; Tamaki, Y.; Murai, M.; Hara, K.; Murata, S.; Arakawa, H.; Tachiya, M. *J. Phys. Chem. B* **2004**, *108*, 3817.

(29) (a) Yamakata, A.; Ishibashi, T.; Onishi, H. *Chem. Phys. Lett.* **2001**, *333*, 271. (b) Yamakata, A.; Ishibashi, T.; Onishi, H. *J. Phys. Chem. B* **2001**, *105*, 7258.

(30) Szczepankiewicz, S. H.; Moss, J. A.; Hoffmann, M. R. *J. Phys. Chem. B* **2002**, *106*, 2922.

(31) Yamakata, A.; Ishibashi, T.; Onishi, H. *J. Phys. Chem. B* **2002**, *106*, 9122.

(32) Lewis, N. S. *Annu. Rev. Phys. Chem.* **1991**, *42*, 543.

(33) Baba, R.; Konda, R.; Fujishima, A. *Chem. Lett.* **1986**, 1307.

(34) (a) For very dry, highly pure MeCN, Schumacher and co-worker observed a value for a flat band potential of -2.0 ± 0.1 V vs. NHE. This value is significantly more negative than that determined for TiO_2 in CH_3CN containing H_2O (2 vol%), i.e., -1.11 V vs. NHE. In the present study, although we used fresh CH_3CN (99%), trace amounts of water and other protic impurities affect the flat band potential of TiO_2. Therefore, we assumed E_{CB} and E_{VB} of -1.1 and +2.1 V vs. NHE, respectively. In fact, we observed the one-electron oxidation reactions of several biphenyl derivatives (E_{ox} = 1.39-2.08 V vs. NHE) by the photogenerated holes under identical conditions.[23b] (b) Heinzel, A. B.; Teschner, D. M.; Schumacher, R. *Ber. Bunsen-Ges. Phvs. Chem.* **1981**. *85*. 1117. (c) Schumacher, R.; Teschner, D.; Heinzel, A. B. *Ber. Bunsen-Ges. Phys. Chem.* **1982**, *86*, 1153.

(35) Mohan, H.; Mittal, J. P. *Bull. Chem. Soc. Jpn.* **2001**, *74*, 1649.

(36) Tojo, S.; Tachikawa, T.; Fujitsuka, M.; Majima, T. *Chem. Phys. Lett*. **2004**, *384*, 312.

(37) Tojo, S.; Tachikawa, T.; Fujitsuka, M.; Majima, T. *Phys. Chem. Chem. Phys*. **2004**, *6*, 960.

(38) Haque, S. A.; Tachibana, Y.; Willis, R. L.; Moser, J. E.; Grätzel, M.; Klug, D. R.; Durrant, J. R. *J. Phys. Chem. B* **2000**, *104*, 538.

(39) Barzykin, A. V.; Tachiya, M. *J. Phys. Chem. B* **2002**, *106*, 4356.